ACS APPLIED MATERIALS & INTERFACES

Energy, Environmental, and Catalysis Applications

Anchoring Fe3O4 nanoparticles on carbon nanotube for microwave-induced catalytic degradation of antibiotics

Shiyuan Liu, Lefu Mei, Xiaoliang Liang, Libing Liao, Guocheng Lv, Shuaifei Ma, Shiyao Lu, Amr M. Abdelkader, and Kai Xi

ACS Appl. Mater. Interfaces, **Just Accepted Manuscript** • DOI: 10.1021/acsami.8b08280 • Publication Date (Web): 09 Aug 2018

Just Accepted

ACS Publications

is published by the American Chemical Society. 1155 Sixteenth Street N.W., Washington, DC 20036

Anchoring Fe_3O_4 nanoparticles on carbon nanotube for microwave-induced catalytic degradation of antibiotics

Shiyuan Liu,[a] Lefu Mei,[a,*] Xiaoliang Liang,[b] Libing Liao,[a,*] Guocheng Lv,[a] Shuaifei Ma,[a] Shiyao Lu,[c] Amr Abdelkader,[d,e] and Kai Xi[e,*]

[a]Beijing Key Laboratory of Materials Utilization of Nonmetallic Minerals and Solid Wastes, National Laboratory of Mineral Materials, School of Materials Science and Technology, China University of Geosciences, Beijing 100083, PR China E-mail: mlf@cugb.edu.cn; lbliao@cugb.edu.cn

[b]Key Laboratory of Mineralogy and Metallogeny, Guangzhou Institute of Geochemistry, Chinese Academy of Sciences, Guangzhou 510640, PR China

[c]Department of Applied Chemistry, School of Science, MOE Key Laboratory for Nonequilibrium Synthesis and Modulation of Condensed Matter, State Key Laboratory for Mechanical Behavior of Materials, Xi'an Jiaotong University, Xi'an 710049, PR China.

[d]Department of Design and Engineering, Faculty of Science & Technology, Bournemouth University, Poole, Dorset, BH12 5BB, United Kingdom.

[e]Department of Materials Science and Metallurgy, University of Cambridge, Cambridge CB3 0FS, United Kingdom, E-mail: kx210@cam.ac.uk.

ABSTRACT

Microwave induced catalytic degradation is considered amongst the most efficient techniques to remove antibiotic such as chlortetracycline from contaminated water. Described here is a new microwave induced oxidation catalyst based on carbon nanotube decorated uniformly with nanoparticles of Fe_3O_4. The combination of dielectric loss and magnetic loss of the material contributed to its stronger microwave absorption and the ability to produce more "hot spots". These hot spots promoted the oxidation of common antibiotics like chlortetracycline, tetracycline and oxytetracycline under microwave irradiation. Experiments with the addition of scavenger showed that hydroxy radical (•OH) together with superoxide radicals ($•O_2^-$) contributed to the

antibiotics removal as well. The final degradation products included CO_2 and NO_3^- as confirmed by mass spectroscopy and ion chromatography analyses. The results indicated that Fe_3O_4/CNTs was an efficient catalyst for microwave-induced oxidation.

KEYWORDS

Microwave induced oxidation; Catalysts; Nanocomposites; Chlortetracycline; Degradation

1 INTRODUCTION

Antibiotics are types of the antimicrobial that can kill or inhibit the growth of microorganisms (bacteria, fungi, viruses, archaea, protozoa, and microalgae).[1,2] With the increasing use of antibiotics in human and veterinary medicine, there is a serious potential risk to release them as micro-contaminations to soil and water ecosystem. Long-term, chronic exposure to antibiotics residues may directly induce the development of antibiotic-resistant genes.[3,4] Also, antibiotic could contribute to the development of resistant and multi-resistant bacteria, possess direct hazard to both human and animals as well as to the environment.[5-7] Therefore, alongside the plans of prudent use of antibiotics in medicines, it is important also to develop effective treatment technology for the contaminated water or soil.[8]

The removal of antibiotics such as chlortetracycline (CTC), tetracycline (TC) and oxytetracycline (OTC) from natural water was difficult and expensive.[2,9] Conventional wastewater treatment plants were not designed for the removal of antimicrobials.[10-14] Therefore, various techniques have been investigated to remove antibiotics and other antimicrobials from water, including chemical oxidation,[15] biodegradation,[16] membrane bioreactors,[17] photocatalytic degradations.[17,18] However, it was difficult in most of the cases to achieve full degradation of the micropollutants, and some residues were still contaminating the water.[19] In addition, most of the tested methods have harmful side effects such as releasing toxic chemicals to the environment. Compared with other methods, microwave-assisted contaminant degradation can achieve higher removal efficiency without any severe side effects.[20] Also, microwave wastewater treatment processes are rapid, scalable, and environmentally friendly.[21] Moreover, the microwave

processes can be tuned to target specific molecules due to the ability to change the activation energy, frequencies and other operation conditions.[20-22]

The microwave-absorbing materials play an essential role in microwave-induced degradation. Therefore, considerable attention has been devoted to developing highly efficient catalytic materials. The commonly used microwave-absorbing materials can be divided into two categories: dielectric loss materials such as carbon nanotubes (CNTs) and carbon nanofibers (CNFs), and magnetic loss materials such as Fe_3O_4 and cobalt (Co).[23] Carbon materials, as well as metallic nanoparticles, were considered as excellent microwave induced catalyst due to the formation of a significant number of "hot spots" under microwave irradiation (MI). The formation of atomic-scale "hot spots" on the surface of metallic nanoparticles has been proven by SERS analysis.[24] These hot spots are regions with localised heat that can adsorb and decompose the organic pollutants.[23,25] However, carbon nanomaterials suffer from poor selectivity and slow adsorption kinetics.[25] Magnetic lose materials, on the other hand, exhibit strong adsorption strength and fast kinetics, but suffer from the narrow absorption frequency bandwidth.[23] Composites of Fe_3O_4 and carbon materials showed good microwave absorbing performance.[26] Li and his coworkers have reported a composite of CNT and Fe_3O_4 with ultra-low reflection loss (RL) value. Their study showed that the large surface interface introduced by Fe_3O_4 as well as the combination of the permeability and the permittivity enhanced the magnetic loss of the composite. For microwave induced degradation, as compared with microwave absorption, controlling the size of Fe_3O_4 would have a positive effect on the efficiency of the degradation. The smaller particles introduce larger interfaces and contribute more active sites as well as high catalytic activity. However, it is still a challenge to design a microwave induced catalyst that can satisfy the requirements of absorbing frequency bandwidth and absorption strength.[23,26] It was also difficult to control the composition and to engineer porous structures that can maximise the interface between the catalyst and the polluted water.[23,27]

In this study, we used a facial synthesis process to design a microwave induced catalyst by controlling the growth of Fe_3O_4 particles on the surface of CNTs (Fig 1). By partially oxidising the CNT, the ferrous oxide source was directed toward the hydroxyl groups on the surface of the nanotubes, resulting in a homogenous disruption of the iron precursors. The directed deposition prevented the aggregation of the nanoparticles. Due to the strong covalent interaction between the

oxide surface groups and the iron precursor, it was possible to remove any excess amount of iron source through a subsequent aggressive washing step, which helped to maintain the size of the particles at the range of 3 to 8 nm. The resulted composite has a porous structure with a high specific surface area that facilitated the interaction between the catalyst and the unwanted water contamination. The established strong interaction between FeO_3O4 and CNT promoted the regeneration of the catalyst and extended its lifecycle. By taking CTC as an example, we showed that the new composite has a high removal efficiency of antibiotics in microwave degradation system. The degradation mechanism of CTC using catalyst-induced microwave was also investigated.

2 EXPERIMENTAL SECTION

1.1. Materials.

The materials used for the syntheses of Fe_3O_4/CNTs were ferrous acetate and nitric acid (Analytical grade, purchased from Beijing Chemical Industry Co.), and multi-walled carbon nanotubes (Purchased from Aladdin Industrial Co.). Ethyl alcohol (200 proof) was purchased from Sigma-Aldrich and CTC was purchased from Hefei Bomei Biological limited company with a purity of 98%. Isopropanol and benzoquinone, used for the studying of degradation mechanism, were purchased from Beijing Chemical Industry Co. All chemicals referred in this research were obtained from commercial sources as reagent grade and used without further purification. Deionised water (15-18.2 MΩ·cm) was used in all experiments. The water was purified by a Smart-RO water system (Shanghai Hetai Instruments Co. Ltd.).

1.2. Synthesis of Fe_3O_4/CNTs.

A two-step process was developed for preparing Fe_3O_4/CNTs composite. The first step includes oxidising CNTs and preparing the intermedium CNTs@Ferrum hydroxy acetic acid (CNTs@FH). The oxidised CNTs were prepared by treating dried CNTs with concentrated nitric acid under sonication, and then the solution was reflux for 4.5 h at 120 °C.[29] The intermedium CNTs@FH was syntheses by the following methods: 40 mg ferrous acetate and 25 mg oxidised CNTs were ultrasonically dispersed into 30 mL pure ethanol to

form a homogeneous dispersion, and then refluxed at 80 °C for 6 h. After cooled to room temperature, the products were centrifuged and washed with ethanol repeatedly and dried at 60 °C. The second step was calcining the prepared CNTs@FH for 2 h at 500 °C in a tube-furnace, using argon as the shielding gas. And the sintered product was denoted as Fe_3O_4/CNTs.

1.3. Characterization.

The structure and crystal phase of synthesised CNTs@FH and Fe_3O_4/CNTs were characterised by X-ray diffraction (XRD) analysis using a CuKα radiation at 40 kV and 100 mA, a scanning speed of 8° 2θ/min, and a step size of 0.02° 2θ from 10° to 70°. Microstructures of the composite, chemical microanalysis, and crystallite-size measurement were analysed using a transmission electron microscope (TEM). Fe_3O_4/CNTs solution (sample powders ultrasonic dispersed in ethanol) was dropped and dried on copper grid-supported carbon films for TEM imaging. Fourier transform infrared spectrophotometer (FT-IR) (Spectrum 100, PerkinElmer, USA) analysis was carried out, and the samples were spread evenly on KBr pellets before scanning.

Microwave absorption properties of Fe_3O_4, CNTs, and Fe_3O_4/CNTs were analysed by the microwave network analyser N5244A (Agilent) in the frequency range of 2 to 18 GHz, using the coaxial wire method in free space. The sample powder (20 wt %) was thoroughly mixed with molten wax (80 wt %), and the mixture was then pressed into toroidally shaped samples. The samples outer diameters were 7.00 mm and inner diameters were 3.04 mm with a thickness of 3 mm.

To measure the catalytic degradation ability, a series of experiments were performed. These experiments were carried out in a condensing device with the initial pH of CTC solution kept at value 6.5. About 0.01 g Fe_3O_4/CNTs was added to 40 mL CTC solution with an initial concentration of 50 mg/L. The reactions were carried out with and without MI in the presence and absence of the catalyst. The solutions after reacting were collected, filtered, and cooled to room temperature before being analysed. The degradation data were obtained in multi-sets of experiments under the same conditions to ensure the effectiveness and the reproducibility.

To investigate the degradation mechanism, CTC solutions before/after degradation were analysed.

The molecular weights of CTC and its degradation products were characterised by high-performance liquid chromatography-mass spectrometer (HPLC–MS, Thermo Scientific). Absolute removal amount of CTC was calculated using UV-Vis spectrophotometer (Precision Scientific Instrument Co. Ltd., Shanghai) at the maximum absorption wavelength of 369 nm. The degradation products were detected by Dionex ICS-3000 Ion Chromatography (IC) System, ICS-3000 Detector/Chromatography Module. The ultraviolet-visible spectra of products from 250 to 450 nm were collected by ultraviolet-visible spectroscopy (Beijing North Temple Instrument Technology Co. Ltd.) with an optical bandwidth of 2.0 nm, a medium scanning speed at an interval of 1 nm, and a response time of 0.2 s. The filtrate obtained by passing the liquid through a 0.22 μm membrane was used to measure the concentrations of total carbon, determined by a TOC-VCPH analyser (Shimadzu, Japan). The total carbon content (TCC) was measured by the TOC-VCPH analyser while the carbon content of CTC was calculated based on the data of UV-Vis spectrophotometer.

3 RESULTS AND DISCUSSION

3.1. Microstructures and Material Properties of Fe_3O_4/CNTs.

The microstructures of CNTs, oxidised CNTs and CNTs@FH were investigated by TEM, and the corresponding images are shown in Fig. 2a, Fig. 2b and Fig. 2c, respectively. The smooth surface of the pristine CNTs became rougher with many obvious defects in the walls after the oxidation. The rough surface helped the Ferrum hydroxy acetic acid (FH) to adhere well to the nanotubes, and a homogeneous uniform coating was obtained as can be seen in Fig. 2c. The EDX analysis (Fig. 2g) showed a uniform distribution of both Fe and C, which further confirmed the homogeneity of the FH layer. TEM images of Fe_3O_4/CNTs (Fig. 2d and Fig. 2e) suggested the formation of the Fe_3O_4 nanoparticles after calcination. The size of the nanoparticles is between 3 to 8 nm in diameter.

Interestingly, the nanoparticles seem to be embedded into the wall of CNT, and a thin layer appears to wrap the nanoparticles. We believe that the high-temperature nature of the calcination played a role in enhancing the interaction between Fe_3O_4 and CNTs, which led to the formation of a conductive network as will be discussed later.[25,27] The controlled heat-treatment during the calcination also helped to maintain equilibrium conditions,[28]

resulting in an excellent crystallinity of the nanoparticles as can be concluded from the clear layered structure in Fig. 2f. The high-resolution TEM images show that the lattice spacing is about 0.251 nm, typically for the d-spacing of (311) in crystal plane of Fe_3O_4. The EDS spectrum of Fe_3O_4/CNTs is illustrated in Fig. 2h. It confirms the uniform loading of Fe_3O_4 nanoparticles on CNTs and the loading amount of Fe_3O_4 was about 22.3 wt%.

The XRD analysis further confirmed the stability of the CNTs structures during the oxidation and calcination. The XRD patterns of synthesised intermediate CNTs@FH, and Fe_3O_4/CNTs (Fig. 3a) show the broad characteristic peaks of CNT at around 26^o 2theta. The other peaks in the Fe_3O_4/CNTs spectrum fit well with that of Fe_3O_4 (JCPDS 75-0033). The particles size of Fe_3O_4 is calculated by the Scherrer's formula and to be 6.65 nm. It is in a good agreement with the particles size showed in TEM images. The absence of the Fe_3O_4 peaks from the CNTs@FH pattern is due to the amorphous nature of the Fe compound. Furthermore, the iron element in CTC solutions before and after degradation was detected by ICP-AES (Table S1). Together with the results of XRD, the absence of iron in solution after CTC degradation confirms the conclusion that Fe_3O_4/CNTs only acted as a catalyst during the degradation process. The FT-IR was used to determine the nature of the interaction between multi-walled CNTs and iron oxide. The obtained FT-IR spectra of CNT, the CNTs@FH precursor, and the Fe_3O_4/CNTs composite after calcination are shown in Fig.3b. The band at 588 cm^{-1} observed for both CNTs@FH and Fe_3O_4/CNTs is associated with the absorption peak of Fe-O,[30] confirming the presence of Fe after refluxing. The stretching band at 1630 cm^{-1} can be assigned to the vibrations of O-H.[31] The intensity of the O-H band of the Fe_3O_4/CNTs is almost the same as that of pristine CNT, suggesting the removal of the OH groups during calcination. The peak at 1400 cm^{-1} belongs to the C–C skeleton vibration of CNTs, which is maintained after the oxidation and calcination processes.[32]

3.2. Microwave Absorption Properties of the Prepared Materials.

For a microwave induced catalyst, the microwave absorbing ability had a significant impact on the degradation efficiency. The microwave absorption properties usually determined by the reflection loss (RL), can be calculated and optimised based on the transmission line theory using the

following equation.[33-36]

$$RL\ (dB)=20 \log | (Z_{in}-Z_0)/(Z_{in}+Z_0) | \quad (1)$$

Where Z_{in} and Z_0 represent the input impedance of the absorber and the impedance of free space. The absorber impedance can be calculated from the following equation:

$$Z_{in}= Z_0(\mu_r/\varepsilon_r)^{1/2}\tanh[j(2\pi fd/c)\ (\mu_r\varepsilon_r)^{1/2}] \quad (2)$$

Where ε_r and μ_r represent the relative complex permittivity and the relative complex permeability, respectively; f stands for the frequency; d is the thickness of toroidal shaped sample and c is the velocity of electromagnetic waves in free space.

Fig. 3c shows the reflection loss curve as a function of the frequency for CNT, Fe_3O_4 and Fe_3O_4/CNTs composite. The RL reaches a minimum value of -19.8 dB at about 2.6 GHz for the Fe_3O_4/CNTs indicating stronger microwave absorption than that of the individual components. The maximum absorption bandwidth (RL <-10 dB, demonstrated over 90% absorption of incident microwave[34]) is significantly boarder for the composite than for the CNT and Fe_3O_4 nanoparticles.

It can be concluded that high imaginary permittivity (ε″) and high imaginary permeability (μ″) reveal the better dissipation ability. While the real parts reveal the ability of a material to store electric(ε′) and magnetic(μ′) energy.[26] The dielectric and magnetic dissipation factors played a key role to evaluate the microwave power lost in a material.[37] The dielectric loss (tan δe = ε″/ε′) for Fe_3O_4/CNTs exhibits an increasing trend from 12 to 18 GHz while magnetic loss tan δμ = μ″/μ′ is descending from 12 to 18 GHz (Fig. 3d). Both of tan δe and tan δμ are maintained at a relatively fixed value from 2 to 12 GHz. The value of the magnetic loss is closer to the dielectric loss in the low-frequency range, indicating better electromagnetic impedance matching. Overall, we can conclude that as for the Fe_3O_4/CNTs, tan δe governs the microwave absorbing ability while tan δμ plays a minor role. Furthermore, due to the presence of magnetic constituents in the as-prepared specimens, μ' and μ'' are around 1 and 0, respectively, with only a slight difference. These results suggest that Fe_3O_4/CNTs possess low magnetic loss ability.[33,36-38] The dielectric and magnetic loss has a different trend of variation. The value of the magnetic loss is higher than that of the dielectric loss, indicating that the later contributes most to enhancing microwave absorption properties of Fe_3O_4/CNTs. The minimum RL of Fe_3O_4/CNTs is

−39.27 dB with a thickness of 2 mm at 12.41 GHz. The improved microwave absorbing behaviour of Fe_3O_4/CNTs can be attributed to the multiple interfacial polarisations between Fe_3O_4 nanoparticles and CNTs, as well as the impedance matching between the material and space.[33,34] Also, the electromagnetic impedance matching is conducive for more microwaves entering inside the material rather than reflecting, resulting in more efficient absorption.

3.3. Degradation of CTC Using Fe_3O_4/CNTs as Catalyst.

Considering the excellent microwave absorption properties of Fe_3O_4/CNTs, one could expect the composite to work well as a catalyst for induced degradation of a wide array of antibiotics.[39] To proof this concept, we have selected CTC as an example of antibiotics and investigated its degradation using Fe_3O_4/CNTs as the catalyst. Although pure MI can remove some CTC (Fig. 4a), the degradation is limited, and the decomposition products have relatively higher molecular weight (Fig. S1, S2). The addition of Fe_3O_4/CNTs significantly improves the efficiency of degradation, particularly under a shorter reaction time. The CTC removal reached a maximum of 185 mg/g within 15 min when the MI was applied in the presence of Fe_3O_4/CNTs. The removal efficiency increased to 93% after 30 min of irradiation. To demonstrate the synergistic effect of CNTs and Fe_3O_4 in the composite, we run a control experiment in which Fe_3O_4 powder and CNTs were physically mixed. The results are shown in Fig. 4a indicates that the physical mixing catalyst has much lower degradation efficiency than the Fe_3O_4/CNTs composite, further confirming the enhancement of the absorption properties of the composite. The TCC in solution decreases with increasing the reaction time (Fig. 4b), suggesting the formation, and emission, of carbon gases such as CO_2. The TCC value is higher than the carbon content of CTC, suggesting that CTC has been disintegrated into smaller organic molecules and then decomposed into inorganic carbon gases. The intensity of the absorption spectrum gradually decreases, indicating progressive CTC removal under MI (Fig. 4c).

UV spectroscopy was used to investigate the kinetics of degradation. The fitting result diagram (Fig. 4d) shows that the microwave induced catalyst degradation, as well as microwave degradation, follow a pseudo-second-order kinetic model. The kinetic coefficient of the degradation reaction is almost three times higher when the catalyst was added (k=0.0376

compared to k=0.0113 without catalyst). The degradation kinetics is significantly higher than that reported in the literature for other antibiotics removal methods as summarised in Table S2 and Fig. 4i.

We have conducted a series of experiments to optimise the process parameters. We investigated the effect of the initial concentration of antibiotic, microwave power, and initial pH on the degradation.[22,40,41] In general, increasing the concentration of CTC resulting in a decrease of the extent of the degradations as can be concluded from Fig. 4e. Increasing the power of the microwave, on the other hand, accelerates the degradation (See Fig. 4f) due to the formation of more "hot spots" or "hot spots" with higher temperatures.[40-44] As a microwave induced catalyst, there is a relationship between microwave absorbing ability and the degradation efficiency. Compared with other catalysts reported before,[42,43] Fe_3O_4/CNTs in this work exhibited lower RL as well as higher degradation efficiency. The higher removal efficiency of CTC was achieved at a pH value close to neutral (Fig.4g), which can be explained by considering the pK_a values. CTC possesses three pK_a values: $pK_{a1} = 3.30$, $pK_{a2} = 7.44$, $pK_{a3} = 9.27$.[45] When the pH of the solution is higher than the pK_{a3}, CTC transforms to iso-chlortetracycline (ICTC).[46,47] Degradation of ICTC using microwave absorbing catalyst has been reported to be slow due to the lack of the phenolic diketone system at several carbon atoms.[46]

To increase the economic aspects of the process, we have also investigated the ability to recycle the Fe_3O_4/CNTs composite. Fig. 4h showed the microwave degradation of CTC using regenerated Fe_3O_4/CNTs composite. Only a slight decrease (9.5 %) is observed in the CTC removal capacity than that recorded when the fresh catalyst was used, indicating the efficient recycling of the catalyst.[48]

3.4. Possible Degradation Mechanism with the Presence of Catalyst under MI.

To confirm the catalytic effect of the Fe_3O_4/CNTs composite, we have run a couple of controlled experiments in which CTC was subjected to MI without the catalyst. The results of the controlled experiments are illustrated in Fig. S1. The removal efficiency of the CTC is three times higher in the presence of the nanocomposite catalyst. The mechanism of the removal is discussed in the following section. There are two general mechanisms by which the CTC molecules can be removed from the solution under MI. The first is the direct pyrolysis where the CTC molecules

decompose (or pyrolyse) by the effect of heating only. The MI causes heterogeneous localised heating, known as the "hot spots", where the temperature could reach 1200 ^{o}C, on the surface of the CNT. It has been reported that this localised heating is enough to pyrolysed H_2O molecules into hydroxyl radical (•OH) and hydrogen radical (•H) around the “hot spots”. CTC molecules can also pyrolyse around the “hot spots” in a similar way. The second removal mechanism is based on the reaction between CTC and highly reactive oxygen species generated on the catalyst under MI. The adsorbed O_2 on the surface of the catalyst reduced to superoxide radicals ($\bullet O_2^-$) which then can react with water to produce hydroxy radical (•OH). Both $\bullet O_2^-$ and •OH are known to be strong oxidative species that react with the active sites in CTC to form inorganic compounds and carbon gases. The indirect removal mechanism can be surmised by equations (3) to (6).[42]

$$H_2O\ (MI) \rightarrow \bullet OH + \bullet H \quad (3)$$

$$2 \bullet H + 2O_2 \rightarrow \bullet O_2^- + 2 \bullet OH \quad (4)$$

$$2 \bullet O_2^- + 2 H_2O \rightarrow 2 \bullet OH + 2 OH^- + O_2 \quad (5)$$

$$\bullet OH + \bullet O_2^- + CTC\ (TC, OTC) \rightarrow \text{inorganic compounds.} \quad (6)$$

In order to determine the most effective oxidative species in the microwave degradation of antibiotics, we conduct a set of control experiments. For investigating the effect of $\bullet O_2^-$, we have added 1 mmol of benzoquinone (a quencher for O_2^-) to the antibiotics solutions. Similarly, we added IPA (a scavenger for •OH) to the solutions in another set of experiments. The concentration of the molecules before and after the microwave treatment was calculated using UV spectroscopy. For the three tested antibiotics (CTC, TC and OTC), the degradation efficiency significantly reduced after adding the scavengers as can be seen from Fig 5a. It is also clear that the effect of the ($\bullet O_2^-$) scavenger is more pronounce than the(•OH) scavenger. Taking CTC as an example, the level of antibiotic removal is almost the same before and after adding IPA (~167 mg/g) but drops to 135 mg/g in the presence of BQ. These results suggest that ($\bullet O_2^-$) is the dominant active species in the oxidation of the CTC.[49-51] Nevertheless, the results of the scavengers control experiments proved that the mechanism of removing CTC is, at least partially, through the oxidation reaction

We have also investigated the final product of the microwave degradation processes of CTC. The gas resulted from the process was passed through 80 mL $Ba(OH)_2$ saturated solution. The solution turned cloudy and white precipitate was observed at the bottom of the solution container (see the inset of Fig 5b). In comparison, there was no visible precipitate for gas coming out of a control

experiment were no CTC was added to the solution. The XRD analysis proved that the white precipitate was $BaCO_3$; thus, we could conclude that the produced gas contains CO_2 (Fig. 5b). We have also analysed the CTC solution before and after the MI using IC (Table S3). The appearance of NO_3^- in solution after the degradation indicated that CTC was decomposed into a nitrogen-containing compound beside CO_2 and H_2O.

The degradation process was further investigated using HPLC-MS. Fig. 6a shows the HPLC spectrum for CTC solution (50 mg/L), and the corresponding MS image is displayed in Fig. S2. The HPLC spectrum of the solution after 30 min of microwave treatment in the absence of the catalyst is illustrated in Fig. 6b. Clearly, MI could partially decompose CTC even without a catalyst. However, the decomposition is not complete. The HPLC-MS detected compounds formed during microwave treatment with relatively large molecular weight. The m/z value of these compounds are 327, 344, 445, and 477 and the predicting molecular formulas are $C_{18}H_{13}O_5$, $C_{18}H_{15}O_6$, $C_{22}H_{24}N_2O_8$, $C_{22}H_{21}ClN_2O_8$, $C_{22}H_{23}ClN_2O_8$. The results of the HPLC-MS indicate that fragmentations of CTC yielded ions with an m/z value of 445 on the loss of Cl, which further fragmented to the ions with an m/z value of 344 on the loss of CO, NH_3 and to the ion with an m/z value of 327 on the loss of H_2O. The exact structures of these compounds could not be identified in this study and further work still required for a more detailed structures analysis. Fig. 6c and Fig. 6d showed the HPLC results when the Fe_3O_4/CNTs catalyst was used under MI for 10 min and 30 min, respectively. The corresponding MS image is provided in Fig. S4. Only a small amount of CTC and its degradation products can be detected after 10 min of microwave treatment in the presence of the catalyst. No obvious intermediate could be detected after 30 min of the treatment. Based on these results, it can be concluded that CTC is completely decomposed through the oxidation by (•OH) and ($•O_2^-$) after less than 30 min of MI.[52,53] The degradation process proceeds through the formation of a series of low molecular weight, organic intermediated compounds, which then further oxidize to water, inorganic ions and carbon dioxide.[42,54-56] The overall degraded reaction can be surmised by the following equation:

$$C_{22}H_{23}ClN_2O_8 + O_2 \rightarrow CO_2 + NO_3^- + Cl^- + H_2O \qquad (7)$$

4. CONCLUSIONS

In summary, the microwave absorbing composite with excellent performance, Fe_3O_4/CNTs, was

synthesised via a simple reflux and calcination method. The mechanism of microwave absorption was systematically studied, which identified the role of the catalyst. Under the MI, "hot spots" formed on the surface of the catalyst, which helped the reduction of the adsorbed molecular oxygen into (•OH) and ($•O_2^-$). As an oxidation catalyst, the Fe_3O_4/CNTs was able to remove 185 mg/g of CTC, and the degradation rate (k=0.0376) was much higher than that previously reported. The work also suggested that the degradation process passes through the formation of a series of intermediate compounds before it decomposes entirely to water, NO_3^- and CO_2.

Acknowledgement

This work was financially supported by National Natural Science Foundation of China (51604248), Fundamental Research Funds for the Central Universities (2652016150), Science and Technology Planning Project of Guangdong Province, China (2017B030314175).

Reference

[1] Jeong, J.; Song, W.; Cooper, W.J.; Jung, J.; Greaves, J. Degradation of Tetracycline Antibiotics: Mechanisms and Kinetic Studies for Advanced Oxidation/Reduction Processes. *Chemosphere.* **2010**, 78, 533–540.

[2] Ekrem, A.; Mehmet, Ş.; Ergin, T.; Halil, H.; Mehmet, E. Chlortetracycline Removal by Using Hydrogen Based Membrane Biofilm Reactor. *J. Hazard. Mater.* **2016**, 320, 88–95.

[3] Daghrir, R.; Drogui, P.; Delegan, N.; Khakani, M. Electrochemical Degradation of Chlortetracycline Using N-Doped Ti/TiO_2 Photoanode Under Sunlight Irradiations. *Water Res.* **2013**, 47, 6801-6810.

[4] Rahman, M.F.; Yanful, E.K.; Jasim, S.Y. Occurrences of Endocrine Disrupting Compounds and Pharmaceuticals in the Aquatic Environment and Their Removal from Drinking Water: Challenges in the Context of the Developing World. *Desalination* **2009**, 248, 578–585.

[5] Baquero, F.; Martínez, J.L.; Cantón, R. Antibiotics and Antibiotic Resistance in Water Environments. *Curr. Opin. Biotechnol.* **2008**, 19, 260–265.

[6] Gomez-Pacheco, C.V.; Sanchez-Polo, M.; Rivera-Utrilla, J.; Lopez-Penalver, J. Tetracycline Removal from Waters by Integrated Technologies Based on Ozonation and Biodegradation. *Chem. Eng. J.* **2011**, 178, 115–121.

[7] Mozaz, S.R.; Chamorro, S.; Marti, E.; Huerta, B.; Gros, M.; Melsió, A.S.; Borrego, C.M.; Barceló, D.; Balcázar, J.L. Occurrence of Antibiotics and Antibiotic Resistance Genes in Hospital and Urban Wastewaters and Their Impact on the Receiving River. *Water Res.* **2015**, 69, 234–242.

[8] Thi, V.H.T.; Lee, B.K. Great Improvement on Tetracycline Removal Using ZnO Rod-Activated Carbon Fiber Composite Prepared with a Facile Microwave Method. *J. Hazard. Mater.* **2017**, 324, 329–339.

[9] Fernandes, A.; Oliveira, C.; Pacheco, M.J.; Ciríaco, L. Anodic Oxidation of Oxytetracycline: Influence of the Experimental Conditions on the Degradation Rate and Mechanism, J. Electrochem. *Sci. Eng*. **2014**, 4 (4), 203–213.

[10] Andreozzi, R.; Raffaele, M.; Nicklas, P. Pharmaceuticals in STP Effluents and Their Solar Photodegradation in Aquatic Environment. *Chemosphere*. **2003**, 50,1319–1330.

[11] Sumpter, J.P.; Johnson, A.C. Lessons from Endocrine Disruption and Their Application to Other Issues Concerning Trace Organics in the Aquatic Environment. *Environ. Sci. Technol.* **2005**, 39, 4321–4332.

[12] Oturan, N.; Wu, J.; Zhang, H.; Sharma, V.K.; Oturan, M.A. Electrocatalytic Destruction of the Antibiotic Tetracycline in Aqueous Medium by Electrochemical Advanced Oxidation Processes: Effect of Electrode Materials. *Appl. Catal. B-Environ.* **2013**, 140-141, 92-97.

[13] Ahmadiab, M.; Motlaghc, H.R.; Jaafarzadehab, N.; Mostoufid, A.; Saeedie, R.; Barzegarc, G.; Jorfiab, S. Enhanced Photocatalytic Degradation of Tetracycline and Real Pharmaceutical Wastewater Using MWCNT/TiO_2 Nano-composite. *J. Environ. Manage.* **2017**, 186, 55-63.

[14] Salazar-Rábago, J.J.; Sánchez-Polo, M.; Rivera-Utrilla, J.; Leyva-Ramos, R.; Ocampo-Pérez, R. Role of $^1O_2$* in Chlortetracycline Degradation by Solar Radiation Assisted by Ruthenium Metal Complexes. *Chem. Eng. J.* **2016**, 284, 896–904.

[15] Doorslaer, X.V.; Demeestere, K.; Heynderickx, P.M.; Langenhove, H.V.; Dewulf, J. UV-A and UV-C Induced Photolytic and Photocatalytic Degradation of Aqueous Ciprofloxacinand Moxifloxacin: Reaction Kinetics and Role of Adsorption. *Appl. Catal. B-Environ*. **2011**, 101, 540-547.

[16] Shi, Y.J.; Wang, X.H.; Qi, Z.; Diao, M.H.; Gao, M.M.; Xing, S.F.; Wang, S.G.; Zhao, X.C. Sorption and Biodegradation of Tetracycline by Nitrifying Granules and the Toxicity of Tetracycline on Granules. *J. Hazard. Mater.* **2011**, 191, 103-109

[17] Tambosi, J.; Sena, R.; Favier, M.; Gebhardt, W.; José, H.; Schröder, H.F.; Moreira, R. Removal of Pharmaceutical Compounds in Membrane Bioreactors (MBR) Applying Submerged Membranes. *Desalination*. **2010**, 261, 148-156.

[18] Liu, S.; Zhao, X.R.; Sun, H.Y.; Li, R.P.; Fang, Y.F.; Huang, Y.P. The Degradation of Tetracycline in a Photo-Electro-Fenton System. *Chem. Eng. J.* **2013**, 231, 441-448

[19] Figueroa, R.; Leonard, A.; Mackay, A. Modeling tetracycline Antibiotic Sorption to Clays. *Environ. Sci. Technol.* **2004**, 38, 476-483.

[20] Remya, N.; Lin, J.G. Current Status of Microwave Application in Wastewater Treatment-A Review. *Chem. Eng. J.* **2011**, 166, 797–813.

[21] Shuai He; G.-S. Wang; C. Lu; J. Liu; B. Wen; H. Liu; L. Guo, M. S. Cao, Enhanced wave absorption of nanocomposites based on the synthesized complex symmetrical CuS nanostructure and poly(vinylidene fluoride). J. Mater. Chem. A **2013**, 15, 4685-4692.

[22] Zhang, L.; Su, M.M.; Guo, X.J. Studies on the Treatment of Brilliant Green Solution by Combination Microwave Induced Oxidation with $CoFe_2O_4$. *Sep. Purif. Technol.* **2008**, 62, 458-463.

[23] Lu, Y.Y.; Wang, Y.T.; Li, H.L.; Lin, Y.; Jiang, Z.Y.; Xie, Z.X.; Kuang, Q.; Zheng, L.S. MOF-Derived Porous Co/C Nanocomposites with Excellent Electromagnetic Wave Absorption Properties. *ACS Appl. Mater. Inter.* **2015**, 7, 13604-13611.

[24] H. -H. Shin, G. J. Yeon, H.-K. Choi, S.-M. Park, K. S. Lee, Z. H. Kim, Frequency-Domain Proof of the Existence of Atomic-Scale SERS Hot-Spots. *Nano Lett.* **2018**, 18, 262−271.

[25] X.M. Duan, M.C. Xiao, S. Liang, Z.Y. Zhang, Y. Zeng, J.B. Xi, S. Wang, Ultrafine Palladium Nanoparticles Supported on Nitrogen-Doped Carbon Microtubes as a High-Performance Organocatalyst. *Carbon* **2017**, 119, 326-331.

[26] N. Li, G.W. Huang, Y.Q. Li, H.M. Xiao, Q.P. Feng, N. Hu, S.Y. Fu, Enhanced Microwave Absorption Performance of Coated Carbon Nanotubes by Optimizing the Fe_3O_4 Nanocoating Structure. *ACS Appl. Mater. Interfaces* **2017**, 9(3), 2973-2983.

[27] Z.Y. Fan, J. Liang, W. Yu, S.J. Ding, S.D. Cheng, G. Yang, Y.L. Wang, Y.X. Xi, K. Xi, R V. Kumar, Ultrathin NiO nanosheets anchored on a highly ordered nanostructured carbon as an enhanced anode material for lithium ion batteries. *Nano Energy* **2015**, 16, 152-162.

[28] Shan, Y.; Gao, L. Formation and Characterization of Multi-Walled Carbon Nanotubes/Co_3O_4 Nanocomposites for Supercapacitors. *Mater. Chem. Phys.* **2007**, 103, 206–210.

[29] Tsang, S.C.; Chen, Y.K.; Harris, P.; Green, M.L. A Simple Chemical Method of Opening and Filling Carbon Nanotubes. *Nature*. **1994**, 372,159.

[30] Pu, Z.J.; Zhou, X.F.; Yang, X.L.; Jia, K.; Liu, X.B. One Step Grafting of Iron Phthalocy Anine Containing Flexible Chains on Fe_3O_4 Nanoparticles Towards High Performance Polymer Magnetic Composites. *J. Magn. Magn. Mater.* **2015**, 385, 368–376.

[31] Zhang, Z.H.; Xu, Y.; Ma, X.P.; Li, F.Y.; Liu, D.N.; Chen, Z.L.; Zhang, F.Q.; Dionysiou, D.D. Microwave Degradation of Methyl Orange Dye in Aqueous Solution in the Presence of Nano-TiO_2-Supported Activated Carbon (Supported-TiO_2/AC/MW). *J. Hazard. Mater.* **2012**, 209–210, 271–277.

[32] Hussain, S.T.; Gilani, S.R.; Ali, S.D.; Bhatti, H.S. Decoration of Carbon Nanotubes with Magnetic $Ni_{1-x}Co_xFe_2O_4$ Nanoparticles by Microemulsion Method. *J. Alloys. Comp.* **2012**, 544, 99-104.

[33] Wang, X.Y.; Mei, L.F.; Xing, X.B.; Liao, L.B.; Lv, G.C.; Li, Z.H.; Wu, L.M. Mechanism and Process of Methyleneblue Degradation by Manganese Oxides Under Microwave Irradiation. *Appl. Catal. B-Environ.* **2014**, 160–161, 211–216.

[34] G.X. Gao, S.Y. Lu, B.T. Dong, W. Yan, W. Wang, T. Zhao, C.Y. Lao, K. Xi, R V. Kumar, S.J. Ding, Construction of Sandwich-Type Hybrid Structures by Anchoring Mesoporous $ZnMn_2O_4$ Nanofoams on Reduced Graphene Oxide with Highly Enhanced Capability. *J. Mater. Chem. A* **2016**, 27, 10419-10424.

[35] L.Y. Zhu, X.J. Zeng, M. Chen, R.H. Yu, Controllable Permittivity in 3D Fe_3O_4/CNTs Network for Remarkable Microwave Absorption Performances. *RSC Adv.*, **2017**, 7, 26801-26808.

[36] J.R. Liu, M. Itoh, K.I. Machida, Electromagnetic Wave Absorption Properties of α-Fe/Fe_3B/Y_2O_3 Nanocomposites in Gigahertz Range. *Appl. Phys. Lett*. **2003**, 83, 4017–4019.

[37] Jian, X.; Wu, B.; Wei, Y.F.; Dou, S.X.; Wang, X.L.; He, W.D.; Mahmood, N. Facile Synthesis of Fe_3O_4/GCs Composites and Their Enhanced Microwave Absorption Properties. *ACS Appl. Mater. Inter.* **2016**, 8, 6101-6109.

[38] Wu, T.; Liu, Y.; Zeng, X.; Cui, T. T.; Zhao, Y. T.; Li, Y. N.; Tong, G. X. Facile hydrothermal synthesis of Fe_3O_4/C Core-Shell Nanorings for Efficient Low-Frequency Microwave Absorption. *ACS Appl. Mater. Interfaces* **2016**, 8, 7370-7380.

[39] D.F. Zhang, Q. Wang, L.L. Wang, L. Zhang, Magnetically Separable $CdFe_2O_4$/graphene Catalyst and its Enhanced Photocatalytic Properties. *J. Mater. Chem. A* **2017**, 34, 332-342.

[40] Daghrir, R.; Drogui, P.; El Khakani, M.A. Photoelectrocatalytic Oxidation of Chlortetracycline Using Ti/TiO_2 Photo-Anode with Simultaneous H_2O_2 Production. *Electrochim. Acta.* **2013**, 87, 18-31.

[41] Zhang, L.; Liu, X.Y.; Guo, X.J.; Su, M.M.; Xu, T.C.; Song, X.Y. Investigation on the Degradation of Brilliant Green Induced Oxidation by $NiFe_2O_4$ Under Microwave Irradiation. *Chem. Eng. J.* **2011**, 173, 734–742.

[42] Chen, J.; Xue, S.; Song, Y.T.; Shen, M.L.; Zhang, Z.H.; Yuan, T.X.; Tian, F.Y.; Dionysiou, D.D. Microwave-Induced Carbon Nanotubes Catalytic Degradation of Organic Pollutants in Aqueous Solution. *J. Hazard. Mater.* **2016**, 310, 226–234.

[43] Lv, G.C.; Xing, X.B.; Liao, L.B.; An, P.F.; Yin, H.; Mei, L.F.; Li, Z.H. Synthesis of Birnessite With Adjustable Electron Spin Magnetic Moments for the Degradation of Tetracycline Under Microwave Induction. *Chem. Eng. J*. **2017**, 326, 329–338.

[44] Liu, X.Y.; Xu, D.; Zhang, D.F.; Zhang, G.Z.; Zhang, L. Superior Performance of 3 D Co-Ni Bimetallic Oxides for Catalytic Degradation of Organic Dye: Investigation on the Effect of Catalyst Morphology and Catalytic Mechanism. *Appl. Catal. B-Environ.* **2016**, 186, 193–203.

[45] Stephens, C.R.; Murai, K.; Brunings, K.J.; Woodward, R.B. Acidity Constants of the Tetracycline Antibiotics. *J. Am. Chem. Soc.* **1956**, 78, 4155-4158.

[46] Soeborg, T.; Ingerslev, F.; Halling-Sorensen, B. Chemical Stability of Chlortetracycline and Chlortetracycline Degradation Products and Epimers in Soil Interstitial Water. *Chemosphere.* **2004**, 57, 1515-1524.

[47] Weilin L. Shelver; Vincent H. Varel Development of a UHPLC-MS/MS Method for the Measurement of Chlortetracycline Degradation in Swine Manure. *Anal. Bioanal. Chem.* **2012**, 402, 1931–1939.

[48] Chernyak, S.A.; Suslova, E.V.; Ivanov, A.S.; Egorov, A.V.; Maslakov, K.I.; Savilov, S.V.; Lunin, V.V. Co Catalysts Supported on Oxidized CNTs: Evolution of Structure During Preparation, Reduction and Catalytic Test in Fischer-Tropsch Synthesis. *Appl. Catal. A-Gen.* **2016**, 523, 221–229.

[49] Wan, J.; Du, X.; Liu, E.; Hu, Y.; Fan, J.; Hu, X. Z-Scheme Visible-Light-Driven Ag_3PO_4 Nanoparticle@MoS_2 Quantum Dot/Few-Layered MoS_2 Nanosheet Heterostructures with High Efficiency and Stability for Photocatalytic Selective Oxidation. *J. Catal.* **2017**, 345, 281-294.

[50] Y. Zhao, Y. Zhang, A. Liu, Z. Wei, S. Liu, Construction of Three-Dimensional Hemin-Functionalized Graphene Hydrogel with High Mechanical Stability and Adsorption Capacity for Enhancing Photodegradation of Methylene Blue. *ACS Appl. Mater. Inter.* **2017**, 9 (4), 4006-4014.

[51] Zhou, M.; Han, D.; Liu, X.; Ma, C.; Wang, H.; Tang, Y.; Huo, P.; Shi, W.; Yan, Y.; Yang, J. Enhanced Visible Light Photocatalytic Activity of Alkaline Earth Metal Ions-Doped CdSe/rGO Photocatalysts Synthesized by Hydrothermal Method. *Appl. Catal. B: Environ.* **2015**, 172–173, 174-184.

[52] Ahmed, A.; Jibril, B.; Danwittayakul, S.; Dutta. J. Microwave-Enhanced Degradation of Phenol over Ni-Loaded ZnO Nanorods Catalyst. *Appl. Catal. B-Environ.* **2014**, 156–157, 456–465.

[53] Mboula, V.M.; Hequet, V.; Gru, Y.; Colin, R.; Andres, Y. Assessment of the Efficiency of Photocatalysis on Tetracycline Biodegradation. *J. Hazard. Mater.* **2012**, 209–210, 355–364.

[54] Lai, T.; Lee, C.C.; Huang, G.L.; Shu, Y.Y.; Wang, C.B. Microwave-Enhanced Catalytic Degradation of 4-Chlorophenol over Nickel Oxides. *Appl. Catal. B-Environ.* **2008**, 78, 151–157.

[55] Llorca, M.; Rodríguez-Mozaz, S.; Couillerot, O.; Panigoni, K.; Gunzburg, J.; Bayer, S.; Czaja, R.; Barceló, D. Identification of New Transformation Products During Enzymatic Treatment of Tetracycline and Erythromycin Antibiotics at Laboratory Scale by an on-Line Turbulent Flow Liquid-Chromatography Coupled to a High Resolution Mass Spectrometer LTQ-Orbitrap. *Chemosphere.* **2015**, 119, 90–98.

[56] Konstantinou, I.K.; Albanis, T.A. TiO_2-Assisted Photocatalytic Degradation of Azo Dyes in Aqueous Solution: Kinetic and Mechanistic Investigations: A Review. *Appl. Catal. B-Environ.* **2004**, 49, 1–14.

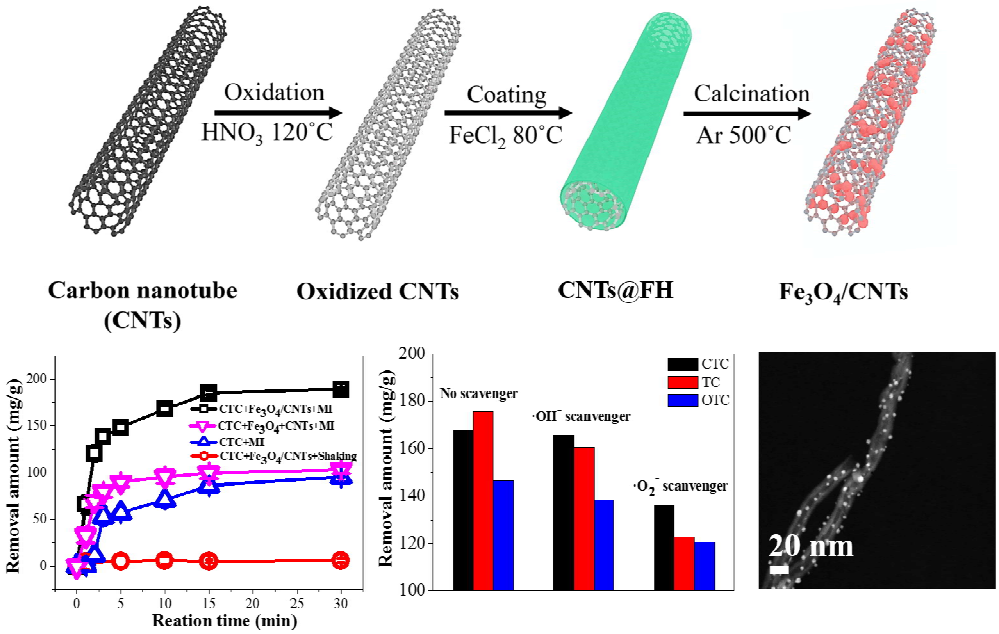

Graphic abstract

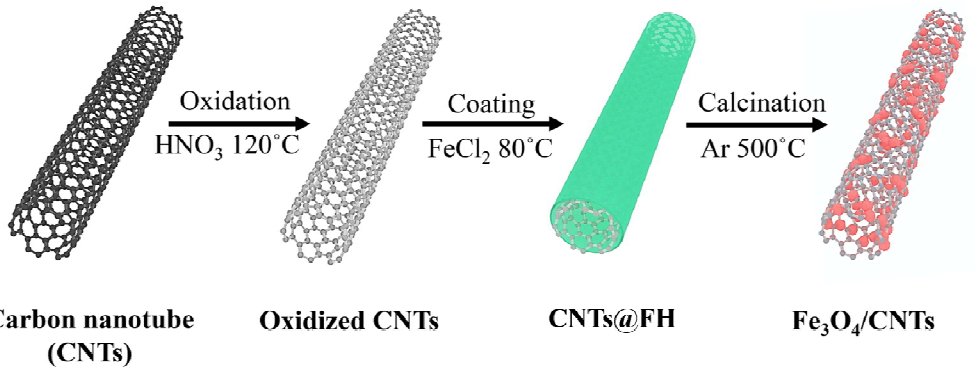

Fig. 1. Formation of the Fe_3O_4/CNTs composite.

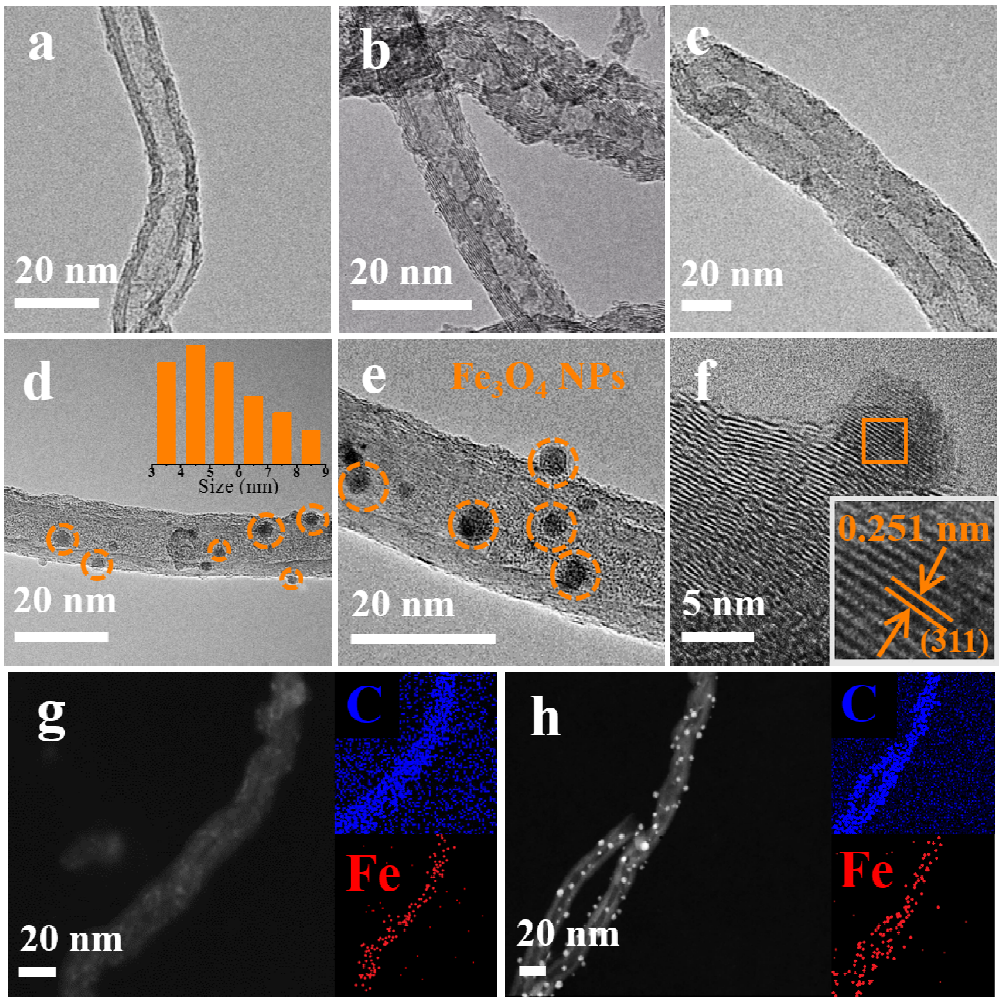

Fig. 2. TEM image of pristine CNTs (a), oxidized CNTs (b), CNTs@FH (c), Fe_3O_4/CNTs (d) and (e), HRTEM image of Fe_3O_4/CNTs using the fast Fourier transform (FFT) (f), EDS element mapping images of CNTs@FH (g) and Fe_3O_4/CNTs (h).

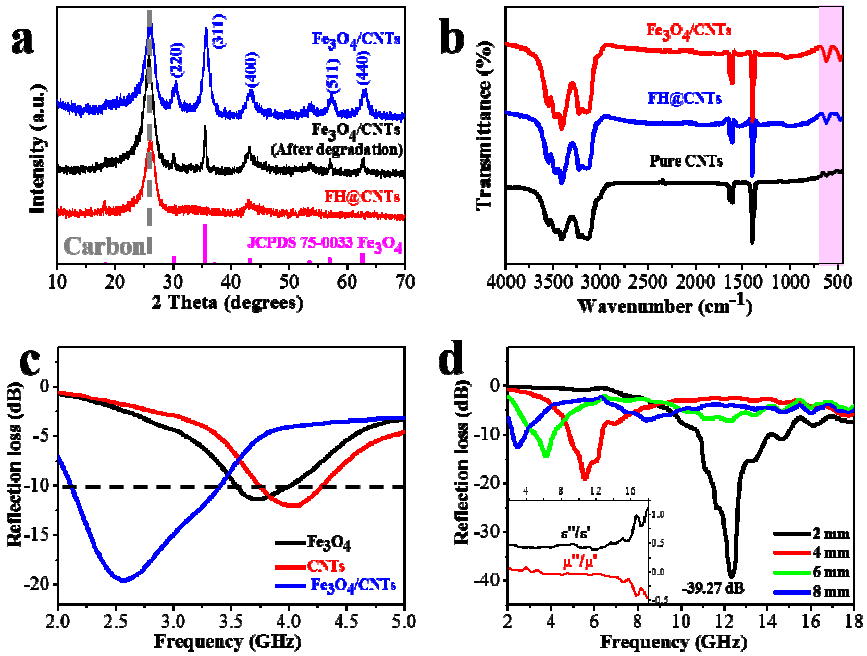

Fig. 3. X-ray diffraction patterns of CNTs@FH, Fe_3O_4/CNTs and Fe_3O_4/CNTs after CTC degradation under MI (a), FT-IR spectrum of oxidized CNTs, CNTs@FH and Fe_3O_4/CNTs (b), reflection absorption rate of CNTs, Fe_3O_4 and Fe_3O_4/CNTs at low frequency (c), reflection absorption rate of Fe_3O_4/CNTs, insert: frequency dependence of relative complex permittivity and relative complex permeability of Fe_3O_4/CNTs(d).

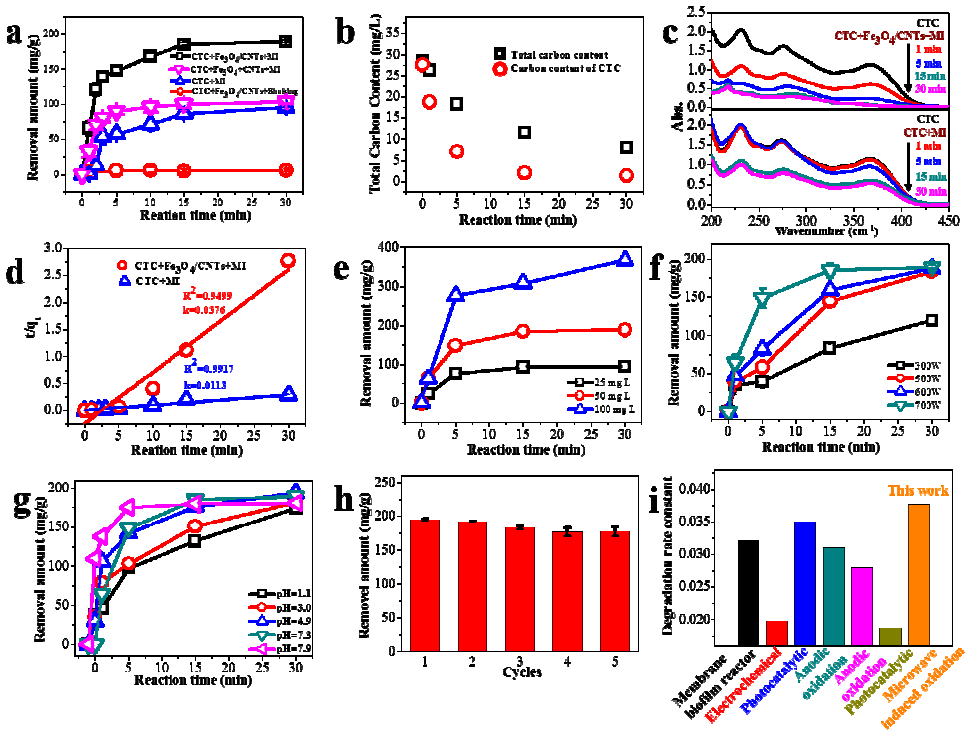

Fig. 4. Residual amount of CTC in the presence and absence of microwave and Fe_3O_4/CNTs (a), total carbon content with Fe_3O_4/CNTs in the presence of microwave (b); UV/Vis spectra of CTC solution with/without Fe_3O_4/CNTs after MI for different time (c), and pseudo-second-order degradation kinetic plots of CTC (d); Effect of initial concentration of CTC (e), microwave power (f), solution pH (g) on the degradation of CTC, cycle stability test for Fe_3O_4/CNTs (h) and comparison of the degradation effects of different treating methods to remove antibiotics (i).

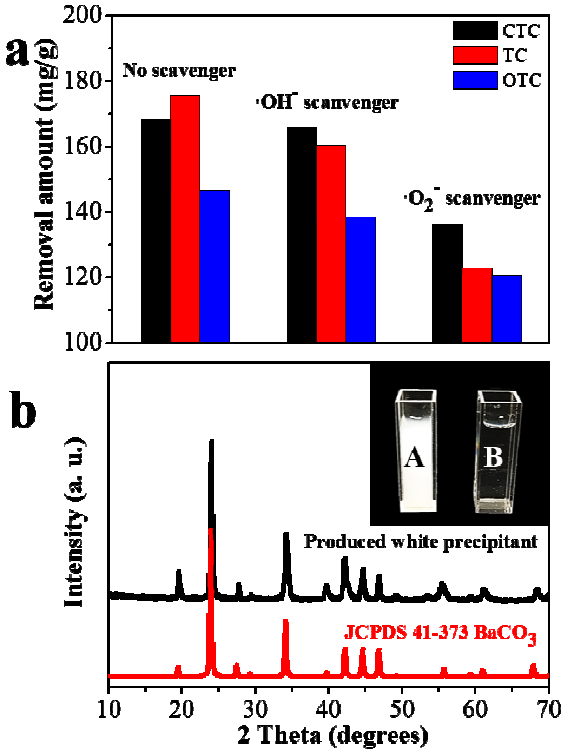

Fig. 5. The effects of scavengers on the degradation of CTC, TC and OTC with Fe_3O_4/CNTs under MI, the reaction time was 30 min (a), XRD patterns of the white precipitation formed in $Ba(OH)_2$ solutions (b), Insert: picture of $Ba(OH)_2$ solutions after treatment. Gas produced by CTC degradation with MI (A) and gas produced by only H_2O with MI (B) passed through the $Ba(OH)_2$ solutions.

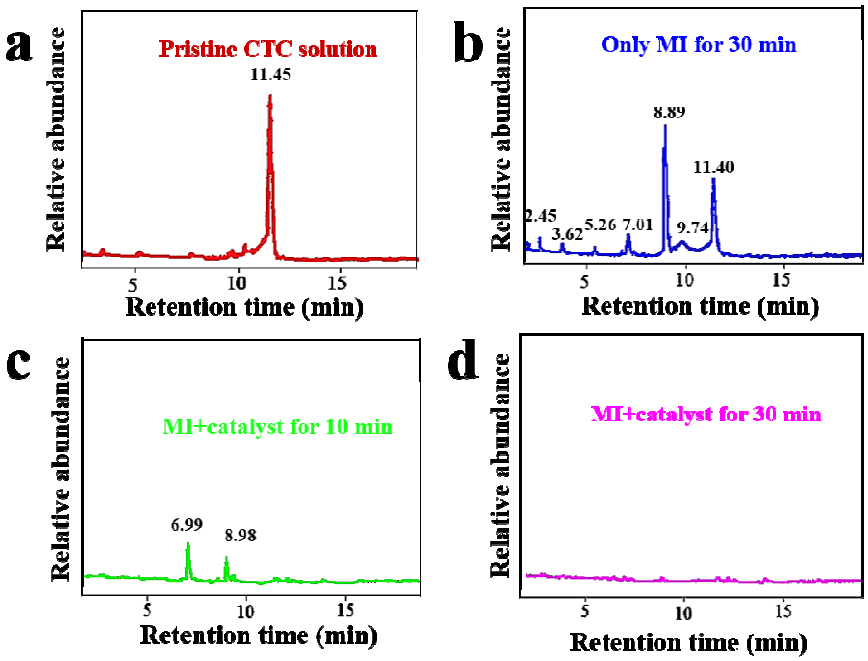

Fig. 6. High-performance liquid chromatography of CTC (a), CTC under microwave radiating for 30 min (b), CTC under microwave radiating using Fe_3O_4/CNTs as a catalyst for 10 min (c) and 30 min (d).